



Contents lists available at SciVerse ScienceDirect

## Chemical Physics Letters

journal homepage: [www.elsevier.com/locate/cplett](http://www.elsevier.com/locate/cplett)

## Structural and optical approach of CdS@ZnS core–shell system

Cristiane W. Raubach<sup>a,\*</sup>, Yuri V.B. de Santana<sup>a</sup>, Mateus M. Ferrer<sup>a</sup>, Valéria M. Longo<sup>b</sup>, José A. Varela<sup>b</sup>, Waldir Avansi Jr.<sup>b</sup>, Prescila G.C. Buzolin<sup>c</sup>, Júlio R. Sambrano<sup>c</sup>, Elson Longo<sup>b</sup><sup>a</sup>INCTMN-UFSCar, Universidade Federal de São Carlos, P.O. Box 676, 13565-905 São Carlos, SP, Brazil<sup>b</sup>INCTMN-UNESP, Universidade Estadual Paulista, P.O. Box 355, 14801-907 Araraquara, SP, Brazil<sup>c</sup>INCTMN-UNESP, Universidade Estadual Paulista, P.O. Box 473, 17033-360 Bauru, SP, Brazil

## ARTICLE INFO

## Article history:

Received 27 January 2012

In final form 22 March 2012

Available online 3 April 2012

## ABSTRACT

An intense red–green photoluminescence (PL) emission was observed, at room temperature, in a CdS@ZnS core–shell system. The PL intensity emission of CdS@ZnS core–shell was strongly superior from that observed in individual CdS and ZnS nanoparticles. In this sense, we reported a comprehensive experimental and theoretical study of the optical behavior of CdS and ZnS nanoparticles (NPs), and CdS@ZnS core–shell system in the light the structural order–disorder conception. We also propose a model where the core and shell interface leads to favorable condition that triggers PL emission in CdS@ZnS core–shell.

© 2012 Elsevier B.V. Open access under the [Elsevier OA license](#).

## 1. Introduction

Wurtzite, CdS and ZnS, are a direct band gap semiconductors with gap energy of 2.42 and 3.7 eV at 300 K, respectively. CdS and ZnS, were one of the first discovered semiconductors [1] and has promising applications in photochemical catalysis [2], gas sensor [3], and optical material [4,5]. The synthesis of CdS and ZnS NPs semiconductors has been the focus of recent scientific research due to their important nonlinear optical properties, luminescent properties, quantum size effect and other important physical and chemical properties [6,7]. These NPs bridge the gap between CdS and ZnS, there by offering the opportunity to study the evolution of interface properties [8,9]. Continuous researches suggest that semiconductor/semiconductor (called as heterostructures) nanocrystals confer a noticeable enhancement in the luminescence and conductive properties due to elimination of surface non-radiative recombination defects [5,10]. Therefore, the design and preparation of composite materials, such as CdSe/ZnS, CdSe/CdS, ZnO/ZnS and CdS/ZnS have been attracted much more research interests [1,5,11].

The study of surfaces and interfaces are expanding areas of scientific studies and technological innovations. In this sense, the development of new heterostructures is still a challenging subject [12]. In the case of this work, the modulation of the properties by tailoring the nucleation of one phase on the surface of other is a critical step. Studies in nanostructured materials indicate that the photoluminescence (PL) property is not only derived from the bulk structure but also controlled by the surface chemical bonds and optical transition in the surface/interface region [13–15]. Several studies performed by our group pointed out the effect of structural

order–disorder in the modulation of the PL emission [16–18]. The surface modification of a wide band gap semiconducting shell around a narrow band gap core can alter the charge, functionality, and reactivity of the materials and consequently enhance the functional properties due to localization of the electron–hole pairs [1,19,20].

In this Letter, we report a comprehensive experimental and theoretical study of the PL emission of CdS or ZnS nanocrystals and CdS@ZnS core–shell system. Experimentally, the samples were characterized by X-ray Diffraction (XRD), UV–vis spectra, Transmission Electron Microscopy (TEM) and PL spectroscopy. Theoretically, first principle calculations were used in sense to investigate the interface between CdS and ZnS that renders the enhanced PL emission. In the light of these results a model of electronic charge and whole transference between the interfaces of CdS@ZnS system is proposed.

## 2. Methods

CdS and ZnS samples (denoted as SAM01 and SAM02, respectively), were synthesized using microwave-assisted solvothermal method, at 453 K during 32 min as described previously [20]. CdS@ZnS (SAM03) core–shell was synthesized using 0.017 mol of CdS powders dispersed in 25 ml of Ethylene Glycol (EG) (solution 01). Separately 0.017 mol zinc ions and 0.03 mol of thiourea were dissolved in 75 ml of EG (solution 02). Then solutions 01 and 02 were mixture in a 120 ml Teflon autoclave and put in the microwave system during 32 min at 453 K. The resulting solution was washed with ethanol several times to neutralize the solution pH ( $\approx 7$ ), and the precipitates were finally collected, and dried at 373 K (5 h). The powders obtained were characterized by XRD collected from 10° to 70° in the 2 $\theta$  range using Cu K $\alpha$  radiation (Rigaku-DMax/

\* Corresponding author.

E-mail address: [cristiane@lic.ufscar.br](mailto:cristiane@lic.ufscar.br) (C.W. Raubach).

2500PC) and TEM JEOL JEM 2100 microscopy, operating at 200 KV. UV–vis spectra were taken using a spectrophotometer of Varian, model Cary 5G (USA) in diffuse reflection mode. PL spectra were collected with a Thermal Jarrel-Ash Monospec monochromator and a Hamamatsu R446 Photomultiplier. The 350.7 nm (2.57 eV) exciting wavelength of a krypton ion laser (Coherent Innova) was used with the output of the laser kept at 200 mW. All measurements were taken at room temperature.

### 3. Results and discussion

XRD patterns were collected for each sample to check the crystalline phase. The XRD (see Supporting Information – S.I.) patterns for the SAM01 could be indexed to CdS crystalline hexagonal in agreement with the respective JCPDS card 65-3414. For the SAM02, the crystalline phase of the as-obtained powder could be indexed to ZnS crystalline hexagonal in agreement with the respective JCPDS card 32-1450 [21]. The existence of a cubic ZnS phase from XRD patterns alone cannot be excluded due to the large similarity between cubic and hexagonal ZnS structures. Thus, these results indicate that ZnS powders processed in a microwave-solvothermal system are crystalline, pure and ordered at long range. Interest to note, that for the SAM03 the mainly peak diffractions observed was related to CdS crystalline phase. Wurtzite has space group  $P6_3mc$ , where each Zn or Cd atom is surrounded by four S atoms at the corners of tetrahedron. Periodic DFT calculations with the B3LYP hybrid functional [22], were performed using the CRYSTAL09 computer code [23]. The atomic centers have been described by an all electron basis set Zn\_86-411d31G [24], for Zn and S\_86-311G\* S [25]. For CdS, the atomic centers have been described by Gaussian basis sets of double-zeta valence polarized (DZVP) [26]. It was modified to be used in CRYSTAL09 code (see S.I.).

As a first step, the optimization of the exponents for the outermost sp and d shells was carried out to minimize the total energy of the structure at experimental parameters. The optimized external exponents are  $\alpha_{sp}(Zn) = 0.14349998$ ,  $\alpha_d(Zn) = 0.73000001$  and  $\alpha_{sp}(S) = 0.38000002$ . The Powell algorithm [27], method was used to perform all basis sets of the optimization procedure. From these optimized exponents, a new optimization procedure of lattice parameters  $a$ ,  $c$  and  $u = (1/3) * (a/c)^2 + (1/4)$  was performed. The calculated and experimental values (given in parentheses) are  $a = 4.30$  (4.14) Å,  $c = 6.96$  (6.71) Å [28] and  $u = 0.377$  (0.376) for CdS and  $a = 3.84$  (3.85) Å,  $c = 6.26$  (6.29) Å and  $u = 0.379$  (0.375) for ZnS. Our results are in good agreement with other theoretical and experimental data [29].

Two periodic models were built from these optimized parameters to represent the ordered ZnS<sub>o</sub> or CdS<sub>o</sub> models and disordered ZnS<sub>d</sub> or CdS<sub>d</sub> models, displacing the Zn or Cd atom, 0.3 Å, in the z-direction, respectively. These models can be useful to represent different degrees of order–disorder in the material, as well as structural defects resulting from Zn to Cd displacements.

Figure 1 presents the TEM images of SAM03. In fact, an expanded image of regions A, in Figure 1a, shows that the SAM03 was formed by a polycrystalline core, Figure 1b. Analyzing an expanded view of region A, inset of Figure 1b, is possible to observe the presence of lattice parameter with about 0.32 nm. This distance is consistent with the (101) plane of the CdS structure, in good agreement with XRD patterns. Additionally, Figure 1c presents an expanded view of region B in Figure 1a suggesting that the observed layer covering the polycrystalline core can be attributed to amorphous ZnS particles, since XRD for SAM03 presents only the CdS crystalline phase (see S.I.).

PL spectra recorded with a 350.7 nm excitation wavelength for the as-obtained samples are shown in Figure 2. The PL spectrum of the SAM01 (CdS) shows a red maximum emission around 655 nm and a greenish maximum emission for SAM02 (ZnS) around 532 nm. The PL spectrum of for the SAM03 presents the maximum emission around 590 nm. The blue-shift observed for the SAM03 compared to SAM01 could be explained for the possible presence of the ZnS disordered shell coated on the surface CdS core, as observed by XRD (see S.I.) and HRTEM images, Figure 1b and c. [30] Another interesting effect in PL spectra is the enhancement in the emission for the SAM03, that can be associated with an inter-band connection between the interface of CdS core and ZnS disordered shell, where ZnS confines the photogenerated electron–hole pairs to the CdS core interface whose is modified by the quantum confinement effect, leading to the passivation of non-radiative transitions, thus enhancing the luminescence intensity [13,19,31]. Thus, the core–shell interface can be monitored directly by PL.

It is well known that the physical and chemical properties of materials are strongly correlated with some structural factors, mainly, the structural order (o)–disorder (d) in the lattice. The materials can be described in terms of the packing of the constituent clusters of the atoms which can be considered the structural motifs. In a typical semiconductor, the intercluster (intermediary range) and intracluster (local range) interaction can occur as a consequence of three different sources: orientation, induction and dispersion interactions [32]. The orientation interaction results from the correlation between the rotation motion of the permanent moments in different  $[CdS_4]_o \dots [ZnS_4]_d$  clusters (intermediate range). The induction interaction occurs due to the polarization of  $[CdS_4]_o$  clusters by the permanent moment of another  $[ZnS_4]_d$  cluster (short range). The dispersion interaction arises from the motion correlation of electrons in neighboring of  $[CdS_4]_o$  and  $[ZnS_4]_d$  clusters (long range). Breaking symmetry process of these clusters, such as distortions, breathings and tilts, create a huge number of different structures and subsequently different materials properties, and this phenomenon can be related to local (short), intermediate and long-range structural order–disorder [33].

Theoretical results point out that a breaking symmetry process in the structure of various semiconductor, associated to order–disorder effects, is a necessary condition for the presence of intermediate

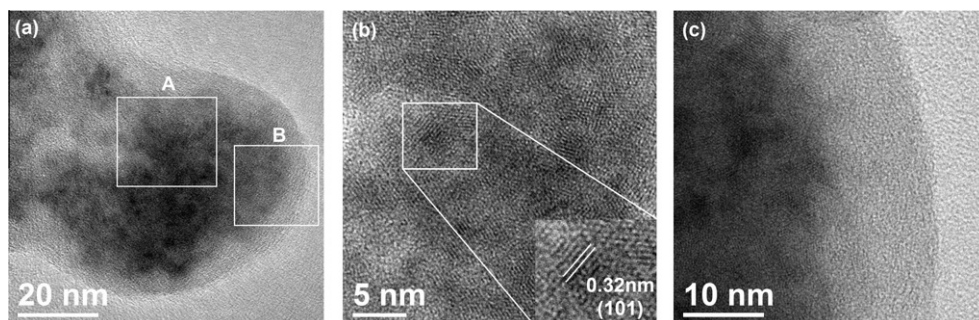
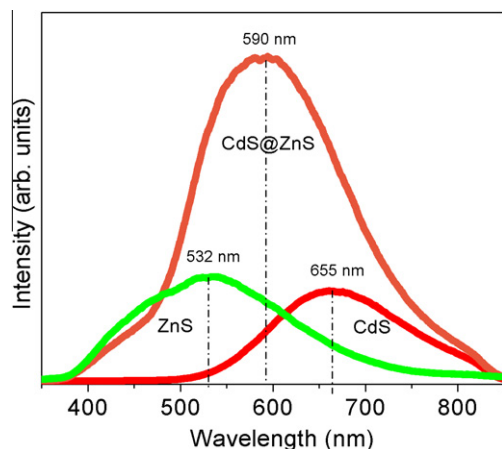


Figure 1. (a) TEM image of SAM03 (CdS@ZnS); (b) HRTEM image of region A; (c) HRTEM image of region B.



**Figure 2.** PL emission spectrum of ZnS, CdS and CdS@ZnS core-shell.

levels in the forbidden band gap [34]. These structural changes can be related to the charge polarization in different ranges that are, at least, manifestations of quantum confinement, when they occur at short and intermediate range undependably of the particle size. The main point for quantum confinement occurs is the presence of discrete levels in the band gap, fact that are not possible with the crystal ore defect are periodic (dispersion interaction) [32].

Table 1 depicts the experimental and theoretical calculated band gap and Fermi energy for the CdS and ZnS ordered and disordered models.

The optical experimental band gap is related to the absorbance and the photon energy by the following Eq. (1) :

$$h\nu\alpha \propto (h\nu - E_{\text{gap}})^{1/2} \quad (1)$$

where  $\alpha$  is the absorbance,  $h$  is the Planck constant,  $\nu$  is the frequency and  $E_{\text{gap}}$  is the optical band gap [35]. The band gap values of CdS, ZnS and CdS@ZnS were evaluated by extrapolating the linear portion of the curve (Supplement material). The entire sample presents a

well-defined inter-band transition with a quasi-vertical absorption front which is typical of semiconductor crystalline materials. The CdS@ZnS core-shell system has two absorption regions, 2.4 and 3.8 eV, which are linked to CdS core and ZnS shell, respectively. The comparison with theoretical results shows a very good concordance between experimental and theoretical results.

Based on both experimental and theoretical findings, we propose a model where the driving force of this dynamic process is the order-disordered effects at intermediate range. In this way we are considering that the core and the shell are neutral and they have the same relevance in terms of electronic structure. This effect can only appear when the intermediate range order-disorder between interfaces, as in this case, core and shell are present.

Figure 3 illustrates an electronic model of CdS ordered core and ZnS disordered shell and CdS@ZnS core-shell interface before the photon arrival.

The model is closely related to the alignment of energy levels of CdS ordered core and ZnS disordered shell. In a first step, electrons split from the electron shell Fermi level ( $E_{Fe}$ )<sub>S</sub> to the core electron Fermi level ( $E_{Fe}$ )<sub>C</sub> and holes split from the core shell Fermi level ( $E_{Fh}$ )<sub>C</sub> to the hole shell Fermi level ( $E_{Fh}$ )<sub>S</sub>. These can also be termed dynamic Fermi levels and are a spontaneous process as the electronic core and shell structure has the electron and whole Fermi energy locates at different Fermi energy but in the same Brillouin zone. The consequence of this dynamic process is the electron population of the valence band (VB) of CdS ordered core and holes migration to shell ZnS conduction band (CB). The final electronic configuration between CdS and ZnS interfaces is interconnected band structures where the core has more electrons and the shell more holes (see S.I.).

During the excitation process, there is a cluster-to-cluster charge transfer (CCCT) [32,33] of electrons from CdS electron populated clusters to ZnS holes populated clusters. The structural and electronic reconstruction of all the possible combinations of clusters in a crystal are essential for the understanding the CCCT process and at least the PL phenomenon. There exist such photoinduced electron-transfer processes where an electron is promoted from an occupied level of the cluster donor to a vacant level of

**Table 1**  
Experimental and theoretical band gap energy and fermi energy of ordered (o) and disordered (d) CdS and ZnS periodic models.

	CdS_o	CdS_d	ZnS_o	ZnS_d	Experimental		
					CdS	ZnS	CdS@ZnS
Gap ( $\Gamma-\Gamma$ ) (eV)	2.66	2.26	3.88	3.42	2.4	3.8	2.4 and 3.8
Fermi energy (eV)	-6.31	-5.96	-5.84	-5.50			

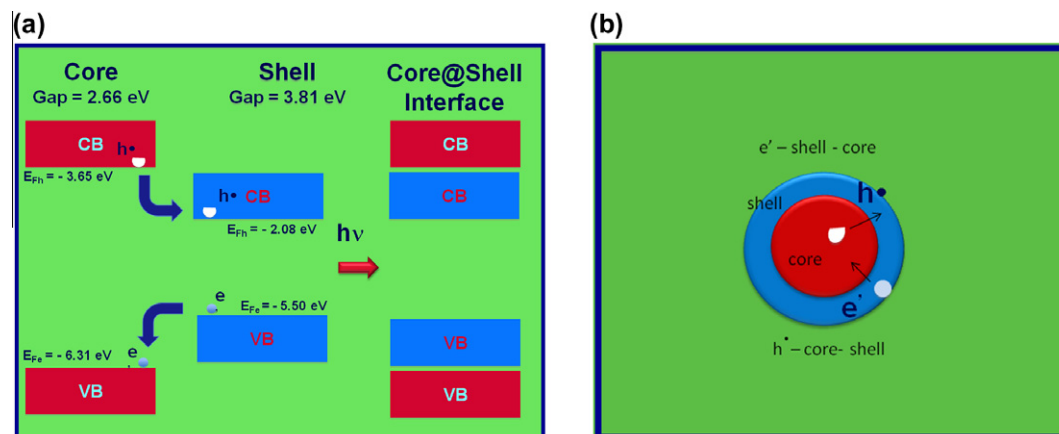


**Figure 3.** (a) Electronic models of CdS@ZnS core-shell interface before the photon arrival (b) illustration of the model of CdS@ZnS core-shell.

the cluster acceptor. The formation of isolated energy levels and the presence of  $[\text{CdS}_3 \cdot V^{\cdot}]$  or  $[\text{ZnS}_3 \cdot V^{\cdot}]$  disordered clusters leads to a substantial recombination between the photoexcited electron and hole during the excitation process. Probably, the ordered  $[\text{ZnS}_4]^{\times} - [\text{CdS}_4]^{\times}$  cluster are activated during the excitation process changing their symmetry going to singlet or triplet excited states, as demonstrated by Gracia et al. [17,36] in perovskite and scheelite structures. In this way, similarly studies have to be done for wurtzite materials to confirm this fact.

#### 4. Conclusions

In summary, CdS@ZnS core-shell system was prepared by an efficient microwave-assisted solvothermal technique and their optical properties were carefully investigated. The XRD patterns and HRTEM images reveal a disordered ZnS layer in the shell and the polycrystalline CdS core. In the light of first principle calculations we propose a model where the unfused layers between core and shell interface renders the favorable condition that triggers PL emission in CdS@ZnS core-shell.

It is clear that controlling the particle size and morphology promotes modulation of advanced properties in heterostructured materials that can be used in future novel technologies. Such novel technologies can in principle explore materials which are not available in the bulk single crystal form, but their figure-of-merit is dramatically dependent on the surface-interface defect states. We believe that the strategy may also be applicable to other materials.

#### Acknowledgements

The authors are thankful for the financial support of Brazilian research financing institutions: CAPES, CNPq and FAPESP. We also thank the Electron Microscopy Laboratory (LME) of the Brazilian National Synchrotron Light Laboratory (LNLS) for the use of its HRTEM microscopy facility.

#### Appendix A. Supplementary data

Supplementary data associated with this Letter can be found, in the online version, at <http://dx.doi.org/10.1016/j.cplett.2012.03.090>.

#### References

- [1] M.A. Malik, P. O'Brien, N. Revaprasadu, *Chem. Mater.* 14 (5) (2002) 2004.
- [2] P.V. Braun, P. Osenar, S.I. Stupp, *Nature* 380 (1996) 325.
- [3] V.L. Colvin, M.C. Schlamp, A.P. Alivisatos, *Nature* 370 (1994) 354.
- [4] W. Hoheisel, V.L. Colvin, C.S. Johnson, A.P. Alivisatos, *J. Chem. Phys.* 10 (1994) 8455.
- [5] J.S. Liu et al., *J. Alloy Compd.* 509 (2011) 9428.
- [6] A.V. Murugan, R.S. Sonawane, B.B. Kale, S.K. Apte, A.V. Kulkarni, *Mater. Chem. Phys.* 71 (2001) 98.
- [7] M.V. Limaye, S. Gokhale, S.A. Acharya, S.K. Kulkarni, *Nanotechnology* 19 (2008) 41.
- [8] L. Biadala, Y. Louyer, P. Tamarat, B. Lounis, *Phys. Rev. Lett.* 103 (2009).
- [9] S. Xu et al., *J. Phys. Chem. C* 115 (2011) 20876.
- [10] S.M. Liu, H.Q. Guo, Z.H. Zhang, R. Li, W. Chen, Z.G. Wang, *Physica E* 8 (2000) 174.
- [11] F. Li, Y. Jiang, L. Hu, L.Y. Liu, Z. Li, X.T. Huang, *J. Alloy Compd.* 474 (2009) 531.
- [12] D. Pergolesi et al., *Nat. Mater.* 9 (2010) 846.
- [13] L. Wang, H.W. Wei, Y.J. Fan, X.Z. Liu, J.H. Zhan, *Nanoscale Res. Lett.* 4 (2009) 558.
- [14] M.J.L. Santos, J. Ferreira, E. Radovanovic, R. Romano, O.L. Alves, E.M. Giroto, *Thin Solid Films* 517 (2009) 5523.
- [15] A. Ishizumi, Y. Kanemitsu, *Adv. Mater.* 18 (2006) 1083.
- [16] M.L. Moreira, J. Andres, V.M. Longo, M.S. Li, J.A. Varela, E. Longo, *Chem. Phys. Lett.* 473 (2009) 293.
- [17] L. Gracia et al., *J. Appl. Phys.* 110 (2011) 043501.
- [18] L.S. Cavalcante, M.F.C. Gurgel, A.Z. Simoes, E. Longo, J.A. Varela, M.R. Joya, P.S. Pizani, *Appl. Phys. Lett.* 90 (2007) 011901.
- [19] R.G. Xie, U. Kolb, J.X. Li, T. Basche, A. Mews, *J. Am. Chem. Soc.* 127 (2005) 7480.
- [20] J.F.A. Oliveira, T.M. Milao, V.D. Araujo, M.L. Moreira, E. Longo, M.I.B. Bernardi, *J. Alloy Compd.* 509 (2011) 6880.
- [21] E.H. Kisi, M.M. Elcombe, *Acta Crystallogr. C* 33 (1983) 1493.
- [22] C.T. Lee, W.T. Yang, R.G. Parr, *Phys. Rev. B* 37 (1988) 785.
- [23] R. Dovesi et al., *CRYSTAL09 User's Manual*, University of Torino, Torino, 2009.
- [24] J.E. Jaffe, A.C. Hess, *Phys. Rev. B* 48 (1993) 7903.
- [25] A. Lichanot, E. Apra, R. Dovesi, *Phys. Status Solidi B* 177 (1993) 157.
- [26] N. Godbout, D.R. Salahub, J. Andzelm, E. Wimmer, *Can. J. Chem.* 70 (1992) 560.
- [27] M.J.D. Powell, *Siam Rev.* 12 (1970) 79.
- [28] S. Wei, S.B. Zhang, *Phys. Rev. B* 62 (2000) 6944.
- [29] H.Z. Zhang, B. Gilbert, F. Huang, J.F. Banfield, *Nature* 424 (2003) 1025.
- [30] Y.J. Hsu, S.Y. Lu, Y.F. Lin, *Adv. Func. Mater.* 15 (2005) 1350.
- [31] S. Kalele, S.W. Gosavi, J. Urban, S.K. Kulkarni, *Curr. Sci.* 91 (2006) 1038.
- [32] L.S. Cavalcante et al., *CrystEngComm* 14 (2012) 853.
- [33] V.M. Longo et al., *J. Phys. Chem. C* 115 (2011) 5207.
- [34] E. Longo et al., *Phys. Rev. B* 69 (2004) 125115.
- [35] D.L. Wood, J. Tauc, *Phys. Rev. B* 5 (1972) 3144.
- [36] L. Gracia, J. Andres, V.M. Longo, J.A. Varela, E. Longo, *Chem. Phys. Lett.* 493 (2010) 141.